Talanta 83 (2010) 344–350

Contents lists available at ScienceDirect

Talanta

journal homepage: www.elsevier.com/locate/talanta

Sorption characteristics and separation of tellurium ions from aqueous solutions using nano-TiO_2

Lei Zhang*, Min Zhang, Xingjia Guo, Xueyan Liu, Pingli Kang, Xia Chen

College of Chemistry, Liaoning University, Shenyang 110036, People's Republic of China

ARTICLE INFO

Article history:
Received 23 July 2010
Received in revised form
14 September 2010
Accepted 18 September 2010
Available online 25 September 2010

Keywords:
Tellurium
Nano-TiO_2
Sorption
Kinetics
Thermodynamics

ABSTRACT

Titanium dioxide nanoparticles (nano-TiO_2) were employed for the sorption of Te(IV) ions from aqueous solution. A detailed study of the process was performed by varying the sorption time, pH, and temperature. The sorption was found to be fast, equilibrium was reached within 8 min. When the concentration of Te(IV) was below 40 mg L^{-1}, at least 97% of tellurium was adsorbed by nano-TiO_2 in the pH range of 1–2 and 8–9. The sorbed Te(IV) ions were desorbed with 2.0 mL of 0.5 mol L^{-1} NaOH. The sorption data could be well interpreted by the Langmuir model with the maximum adsorption capacity of 32.75 mg g^{-1} (20 ± 0.1 °C) of Te(IV) on nano-TiO_2. The kinetics and thermodynamics of the sorption of Te(IV) onto nano-TiO_2 were also studied. The kinetic experimental data properly correlated with the second-order kinetic model (k_2 = 0.0368 g mg^{-1} min^{-1}, 293 K). The overall rate process appeared to be influenced by both boundary layer diffusion and intra-particle diffusion. The mean energy of adsorption was calculated to be 17.41 kJ mol^{-1} from the Dubinin–Radushkevich (D–R) adsorption isotherm at room temperature. Moreover, the thermodynamic parameters for the sorption were estimated, and the ΔH^0 and ΔG^0 values indicated the exothermic and spontaneous nature of the sorption process, respectively. Finally, Nano-TiO_2 as sorbent was successfully applied to the separation of Te(IV) from the environmental samples with satisfactory results (recoveries >95%, relative standard deviations was 2.0%).

1. Introduction

The solid tellurium is a p-type semiconductor and primarily used in semiconductor technology. Besides, it is also used in glass and ceramic industry, as well as metallurgy as an additive to steel and copper to provide machinability. Tellurium, known to be toxic to living biological systems, is regarded as rare, non-essential element, usually occurs at low concentration levels (10^{-6}%). Tellurium can be accumulated in kidney, heart, liver and spleen, and induce the degeneracy of liver and kidney in excess of 0.002 g kg^{-1} [1]. Tellurium is usually determined in a wide range of matrices, e.g., biological, clinical, geological, semiconductor, and metallurgical samples. The determination of tellurium is often a difficult task because of the very low concentration and complex matrices. In most cases a separation process is essential before the determination of tellurium. The most widely used techniques for the separation of trace tellurium include the extraction [2], liquid membrane [3], and microbiological process [4]. Solvent extraction methods, using polar solvents such as tributyl phosphate (TBP), methyl isobutyl ketone (MIBK) trioctylphosphine oxide (TOPO), and di-(2-ethylhexyl) phosphoric acid have been reviewed [5–7]. Solvent extraction methods of Te(IV) recently reported include tris-(2-ethyl hexyl) phosphate [8], 2,3,5-triphenyltetrazolium chloride [9], triphenylarsin oxide and tributyl-phosphine oxide [10]. Most of the extracting agents used in these methods are extremely toxic and hardly suitable for routine analyses.

Nano-TiO_2 as sorbent for separation of trace elements is an increasing interest owing to its effectiveness [11,12]. However, to the best of our knowledge, until now there is no report on the application of nano-TiO_2 for separating Te(IV) ions in aqueous solution.

We want to report here on the optimal conditions for a maximal adsorption of Te(IV) ions from aqueous solutions using nano-TiO_2 in the absence and presence of the different ions. Besides, the adsorption data were fitted to various equations to obtain the equilibrium constants and the kinetics of the adsorption phenomena. The methods were applied for separation of Te(IV) from water and ore samples.

2. Experimental

2.1. Apparatus

Cary 5000 UV–Vis–NIR spectrophotometer (VARIAN) was used for the determination of Te(IV) ions. Mettler Toledo 320-S pH meter Instrument (Shanghai Co. Ltd.) was used for pH measurements. KQ-100 Controllable Serial-Ultrasonics apparatus (Kunshan apparatus

* Corresponding author. Tel.: +86 24 622027809; fax: +86 24 62202380.
E-mail address: zhanglei63@126.com (L. Zhang).

0039-9140/$ – see front matter © 2010 Elsevier B.V. All rights reserved.
doi:10.1016/j.talanta.2010.09.022

company, China) was applied to disperse nano-TiO_2 in solution, operating at an ultrasonic frequency of 20–80 kHz and an output power between 0 and 50 W through manual adjustment. Model TDL80-2B centrifugal machine (Shanghai Anting Scientific Instrument Co., China) was used throughout.

2.2. Materials and reagents

Nano-TiO_2 was purchased from Zhoushanmingri Nanometer Material Co., China and its particle size was about 10–15 nm.

The certified reference material molybdenum ore (GBW07285) was provided by State Technology Supervision Administration (China).

A stock solution of Te(IV) (1.0000 mg mL^{-1}) was prepared by dissolving 1.3030 g of TeO_2 in 10 mL concentrated hydrochloric acid, and then diluting to the desired concentration with 0.6 mol L^{-1} HCl. All reagents, including cetyltrimethyl ammonium bromide (CTMAB, 1%), salicyl fluorescence ketone (SAF, 1.0×10^{-3} mol L^{-1}), sodium acetate, acetic acid, hydrochloric acid and sodium hydroxide were of analytical reagent grade and purchased from Shanghai Xinzhong Chemical Reagent Co., China. Deionized water was used throughout the experiments.

The stock solutions of the various metal ions (mg mL^{-1}) were prepared with their nitrate or chloride salts (≥99.99%) and used to investigate the effects of interfering ions.

2.3. Procedure

2.3.1. Determination of Te(IV)

Aliquots of a stock solution containing 1–12 μg of Te(IV) were transferred into a series of 25 mL volumetric flasks followed by the addition of 1.5 mL of 1.0×10^{-3} mol L^{-1} SAF, 1.0 mL of 1% CTMAB, 5.0 mL of 0.2 mol L^{-1} HAc-NaAc buffer solutions (pH 4.8) and the necessary amount of deionized water. After 10 min, the concentration of Te(IV) was determined using a UV–Vis–NIR spectrometer at wavelength of 535 nm [13].

2.3.2. General adsorption and desorption procedure

The adsorption experiments were carried out using a series of 50 mL flasks containing 15 mg nano-TiO_2 and 10.0 mL of 30.0 mg L^{-1} Te(IV) solution (pH 8.5). If necessary, the pH of the solutions was adjusted by adding HCl or NaOH solution before the addition of nano-TiO_2. After ultrasonic dispersion for 8 min, the solid/liquid phases were separated by centrifuging at 5000 rpm for 5 min. The suspensions were immediately analyzed for the determination of Te(IV) concentration.

The adsorption percentage (*Ads.%*) was calculated based on the following equation:

$$Ads.\% = \frac{(C_i - C_a)}{C_i} \times 100 \quad (1)$$

where C_i and C_a are the initial and the final concentration of Te(IV) in solution phase, respectively.

The adsorbed Te(IV) ions were desorbed from solid phase into aqueous medium with 2.0 mL of 0.5 mol L^{-1} NaOH eluent solution. Then the eluent solution was measured with reference to the adsorption and desorption from blank test.

Adsorption isotherm studies were carried out with initial concentrations of Te(IV) varying between 30.0 and 90.0 mg L^{-1}, the amount of sorbent was kept constant (15 mg) and the experimental temperatures were controlled at 273, 293 and 313 K, respectively. The thermodynamic parameters for the adsorption process were determined at each temperature. An experiment without nano-TiO_2 was carried out confirming that no adsorption occurred on the container wall.

Kinetic experiments were performed using a series of 50 mL flasks containing 10 mg nano-TiO_2 and 10.0 mL of 30.0 mg L^{-1} Te(IV) solution at pH 8.5 in a temperature range of 273–313 K. On regular time intervals, suitable aliquots were taken whereupon the Te(IV) concentration was determined. The rate constants were calculated using the conventional rate expression.

2.3.3. Sample preparation

Portions (1.0000 g) of the certified reference material (GBW07285 molybdenum ore) were decomposed with aqua regia (30 mL), heated until the solution becomes transparent, continuously heated to dryness. Then 2 mL of 9 mol L^{-1} H_2SO_4 solution was added, and the samples were heated to emit white smoke for removal nitrogen oxide. The residue was dissolved with 5 mL of 12 mol L^{-1} HCl, and heated in water bath for 15 min, finally diluted to 50 mL with water and adjusted to pH 8.5.

The industrial wastewater samples were filtrated with a 0.45 μm membrane filter, and then acidified to pH 2.0 for storage. Before determination of Te(VI), 5 mL of 12 mol L^{-1} HCl was added to the wastewater and the spiked water samples. Then the samples were heated in water bath for 15 min for reducing Te(VI). Finally the samples were adjusted to pH 8.5 according to the optimized experiment conditions.

3. Results and discussion

3.1. Selection of nano-TiO_2 sorbent type

The effects of different sorbents on the adsorption behavior for Te(IV) ions in aqueous solutions were studied and listed in Table 1. It was found that nano-TiO_2 (anatase) and nano-TiO_2 (rutile type) were the best sorbents for Te(IV). In order to quantificationally separate Te(IV) from the molybdenum ore sample, nano-TiO_2 (rutile type) was chosen as sorbents for Te(IV) ions in the following experiment. Moreover, the test found that almost no adsorption of MoO_4^{2-} on nano-TiO_2 (rutile type) was observed. So nano-TiO_2 (rutile type) was used as sorbents for Te(IV) ions in the experiment.

3.2. Effect of the amount of sorbent

In order to attain the optimal amount of nano-TiO_2 for the adsorption of Te(IV) ions, 5.0, 10.0, 15.0, 20.0, 30.0, 40.0 mg of nano-TiO_2 were added to a series of 10 mL 30 mg L^{-1} Te(IV) solutions (pH 8.5), respectively, then these solutions were ultrasonically dispersed for 8 min, finally centrifuged. The measured results (Fig. 1) showed that when the amount of nano-TiO_2 exceeded 15.0 mg, the adsorption percentage of Te(IV) on nano-TiO_2 was close to 100%. Therefore, 15.0 mg of the sorbent was the optimum amount for the adsorption of Te(IV).

3.3. Effect of pH

We applied 10 mL of solutions with different concentrations (5 mg L^{-1}–70 mg L^{-1}) of Te(IV) to test the sorption of Te(IV) onto nano-TiO_2 at different pH values. The result was shown in Fig. 2. When the concentration of Te(IV) was less than 40 mg L^{-1}, the

Table 1
Effect of different sorbents on adsorption behavior of Te(IV).

Sorbents	Ads.%/Te(IV)	Ads.%/Mo(VI)
Nano-TiO_2 (anatase type, 10–15 nm)	98.4	82.1
Nano-TiO_2 (rutile type, 10–15 nm)	98.1	0.0
Micron-TiO_2	34.5	0.0
Nano-SiO_2 (20 nm)	1.0	
Nano-Al_2O_3 (γ, 10 nm)	89.3	

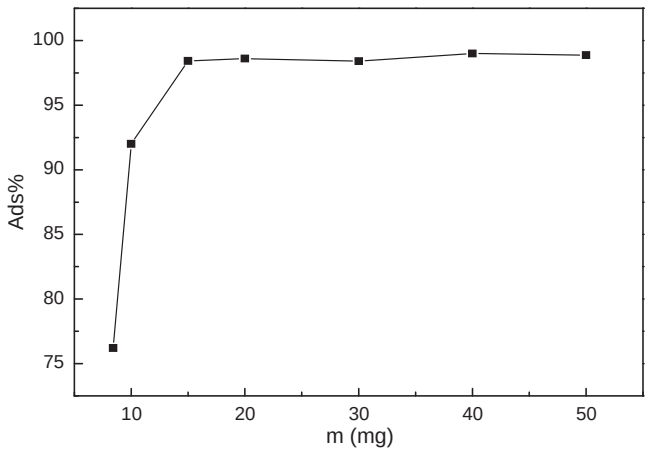

Fig. 1. Effect of nano-TiO_2 amount on the adsorption of Te(IV).

adsorption percentage of Te(IV) was found to be above 97% in the pH range of 1–2 and 8–9. And it was found that Te(IV) ions exist in the forms of deposition at pH 3∼7. At the higher pH the adsorption percentage of Te(IV) decreased with increasing the solution pH, the lowest uptake occurred at pH 13. The maximum adsorption was obtained in the pH range of 1–2 and 8–9, and pH 8.5 was chosen for sorption of Te(IV) ions in the experiment.

Te(IV) is sparingly soluble in acid media, insoluble in neutral media, and soluble in alkaline media [14]. At low pH (<2) Te(IV) may exist in the form of $H_3TeO_3^+$. In alkaline media, the most important species are H_2TeO_3 ($Te(OH)_4$) and $HTeO_3^-$ ($TeO(OH)_3^-$). At even higher pH (10–12) TeO_3^{2-} is predominate [15].

TiO_2 suspension is composed of the mixture of positively charged $\equiv TiOH_2^+$ and neutral species of $\equiv TiOH^0$ when its pH is below pH_{IEP} (6.8); when pH is above pH_{IEP}, the primary species of the suspended TiO_2 include the neutral species of $\equiv TiOH^0$ and the negatively charged $\equiv TiO^-$.

Therefore, the adsorption of Te(IV) on TiO_2 can be viewed as the interaction between $Te(OH)_4/HTeO_3^-$ and $\equiv TiOH^0/\equiv TiO^-$ at pH > 6.8. Based on the above discussion, we propose the following reactions to explain the adsorption mechanisms of Te(IV) onto TiO_2 surface. More Te(IV) ions were in the form of TeO_3^{2-} at higher pH values, and there existed electrostatic repulsion between the negative charged sorbents and TeO_3^{2-}, consequently the adsorption percentage of Te(IV) was observed to decrease.

When pH varied from 8.0 to 11.0, the mechanism of tellurium species adsorbed on TiO_2 was complex. Adsorption of Te(IV) may be through the formation of surface complexation reaction as follows:

$$\equiv Ti\text{–}OH + Te(OH)_4 \rightleftharpoons \equiv Ti\text{–}H_nTeO_4^{(4-n-1)-} + H_2O + (3-n)H^+$$

where $n = 0, 1, 2$.

In addition, Te(IV) species adsorbed onto TiO_2 surface also may be through the formation of hydrogen bonds:

$$\equiv TiOH^0 + Te(OH)_4{}^0 \rightleftharpoons \equiv TiOHOHTe(OH)_3$$

$$\equiv TiO^- + Te(OH)_4{}^0 \rightleftharpoons \equiv TiOHOTe(OH)_3{}^-$$

$$\equiv TiOH^0 + TeO(OH)_3{}^- \rightleftharpoons \equiv TiOHOHTe(OH)_2O^-$$

$$\equiv TiO^- + TeO(OH)_3{}^- \rightleftharpoons \equiv TiOHOTeO(OH)_2{}^{2-}$$

3.4. Desorption and enrichment factor

It could be seen from Fig. 2 that the adsorption of Te(IV) obviously decreased at pH > 11.5. For this reason, 15.0 mg of nano-TiO_2 was added to 10 mL of 30 mg L^{-1} Te(IV) solutions. The solutions of various concentrations NaOH were studied for the elution of the retained Te(IV) ions on nano-TiO_2. Then the effect of eluent volume on the desorption of analytes was also studied at the optimum concentration of the eluent (0.5 mol L^{-1} NaOH). The elution percentage (>95%) was obtained with 2.0 mL of 0.5 mol L^{-1} NaOH.

In order to study the effect of the sample volume on the recoveries of Te(IV) ions, Te(IV) was enriched from volumes of 10, 20, 30, 50, 75 and 100 mL of sample solutions containing 300 μg of Te(IV) by the procedure mentioned above. A quantitative recovery (≥95%) was still obtained for the sample volume of 50 mL for Te(IV) ions. In the experiment, a 50 mL of sample solution was adopted and the enrichment factor was 25 with 2.0 mL of 0.5 mol L^{-1} NaOH elution [16].

3.5. Adsorption kinetic model

The kinetics of the sorption of Te(IV) onto nano-TiO_2 was investigated by agitating a 10 mL of solution containing 30 mg L^{-1} Te(IV). Fig. 3 depicts the variation of adsorption capacity with adsorption time. The obtained curves reflect that the adsorption capacity increases until equilibrium is attained around 8 min.

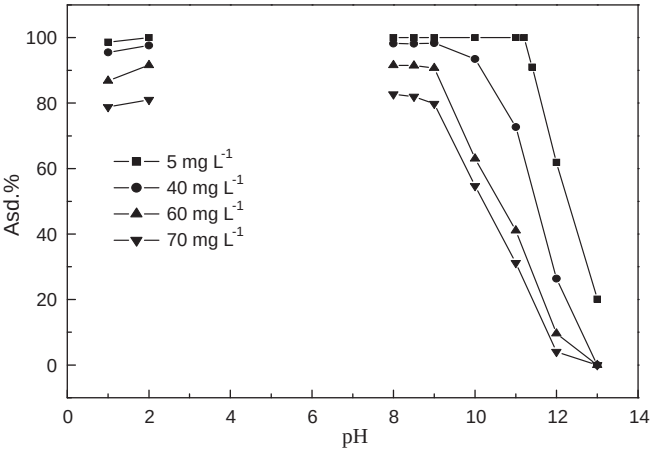

Fig. 2. Effect of pH on the adsorption efficiency of Te(IV) on nano-TiO_2 (15 mg nano-TiO_2; Temp. 20 ± 0.1 °C).

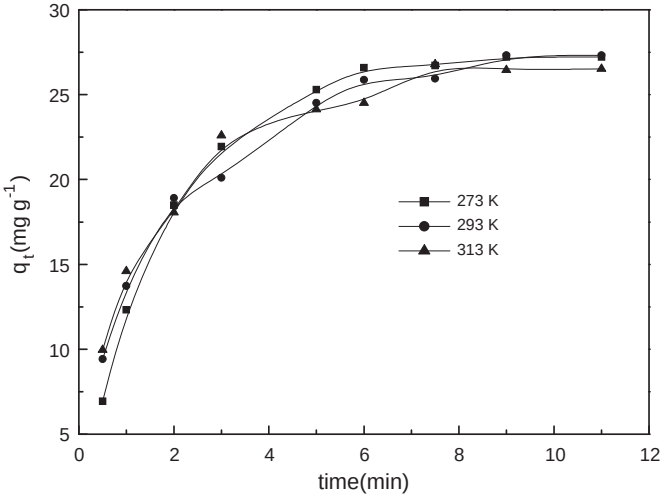

Fig. 3. Adsorption capacity of Te(IV) on nano-TiO_2 versus time at different temperatures (15 mg nano-TiO_2; $C_{Te(IV)}$: 30 mg L^{-1}; pH 8.5).

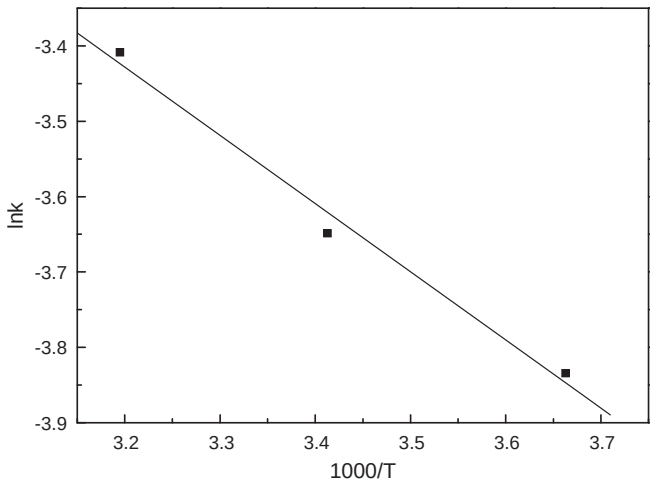

Fig. 4. Plot of ln k versus. 1000/T (the points correspond to 273, 293, 313 K) (15 mg of nano-TiO_2; $C_{Te(IV)}$: 30.0 mg L^{-1}; pH 8.5)

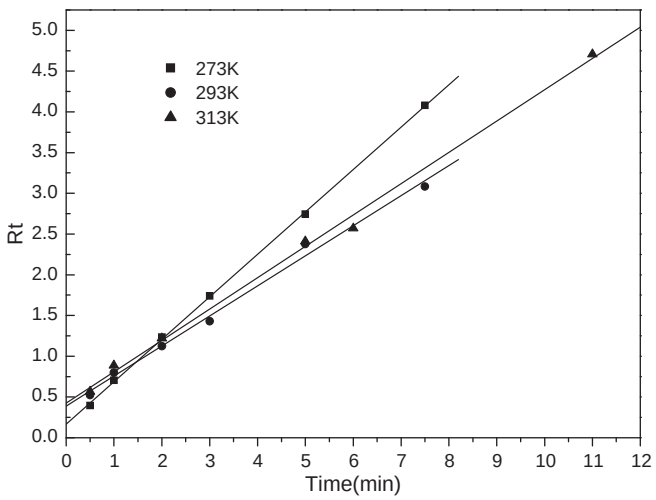

Fig. 5. Plots of Rt versus t for the adsorption of Te(IV) ions on nano-TiO_2 at different temperatures.

In order to investigate the adsorption process of Te(IV) on nano-TiO_2, pseudo-first-order, pseudo-second-order, Richenberg model and Weber–Morris kinetic models were used.

3.5.1. Pseudo-first-order model

The pseudo-first-order equation is given as [17]:

$$lg(q_1 - q_t) = lg\, q_1 - \frac{k_1 t}{2.303} \quad (2)$$

where q_1 and q_t are the amount of Te(IV) adsorbed on the sorbent (mg g^{-1}) at equilibrium and at time t, respectively, and k_1 is the rate constant of the first-order adsorption (min^{-1}). The values k_1 for Te(IV) adsorption on nano-TiO_2 were determined from the plot of lg $(q_1 - q_t)$ against t.

3.5.2. Pseudo-second-order model

The pseudo-second-order model is represented as [17]:

$$\frac{t}{q_t} = \frac{1}{k_2 {q_2}^2} + \frac{t}{q_2} \quad (3)$$

where k_2 is the rate constant of the second-order adsorption (g mg^{-1} min^{-1}). The straight-line plots of t/q_t versus t have been tested to obtain rate parameters.

The batch kinetic data were fitted to both first-pseudo and second-pseudo order models. Both models adequately described the kinetic data at 95% confidence level. The results of the kinetic parameters for Te(IV) adsorption are listed in Table 2. Based on the correlation coefficients the adsorption of Te(IV) is best described by the pseudo-second-order model.

Furthermore, it was possible to calculate the activation energy (E_a) for the adsorption employing the Arrhenius equation based on the obtained rate constants presented in Table 2. From Fig. 4 a value of E_a for Te(IV) adsorption on nano-TiO_2 was obtained to be 7.52 kJ mol^{-1}.

3.5.3. Richenberg model

The rate-controlling step in ion exchange or adsorption is usually either liquid film diffusion or particle diffusion. In order to ascertain the rate-controlling step, the following equations were applied to the adsorption kinetic data [18,19].

For film diffusion

$$Rt = -\ln(1 - F) \quad (4)$$

For intra-particle diffusion

$$Bt = -\ln(1 - F) - 0.4977 \quad (5)$$

where $F = q_t/q_e$; q_t and q_e are the amounts of Te(IV) adsorbed on nano-TiO_2 (mg g^{-1}) at time t (min) and at equilibrium time (min), respectively; R is the rate constant for film diffusion; $B = \pi^2 D_i/r^2$ (D_i is the inter-diffusion coefficient and r is the particle radius). Plots of $-\ln(1-F)$ and Bt versus time, t, according to Eqs. (4) and (5), are shown in Figs. 5 and 6, respectively. Linear correlations were obtained for $-\ln(1-F)$ versus t (Fig. 5). Since the curves do not pass through the origin, the film diffusion is not involved in the kinetics of Te(IV) adsorption on nano-TiO_2. Fig. 6 depicts the linear correlation between Bt versus t. Here, since the curves nearly passed through the origin, the intra-particle diffusion may be the rate-controlling step [19].

3.5.4. Weber–Morris kinetic model

Adsorption kinetic data were further processed to confirm whether intra-particle diffusion is the rate limiting step and to find out the rate determining parameter for intra-particle diffusion. For such purpose Weber–Morris equation was applied:

$$q_t = K_d t^{1/2} + I \quad (6)$$

K_d is the rate constant for intra-particle diffusion. Values of I give an idea about the thickness of the boundary layer, i.e., the larger the intercept, the greater the boundary layer effect will be [20]. Plots of the amount of Te(IV) adsorbed against the square

Table 2
Kinetic parameters for Te(IV) adsorption on nano-TiO_2 at the different temperatures.

T (K)	Pseudo-first-order model			Pseudo-second-order model		
	k_1 (min^{-1})	q_1 (mg g^{-1})	r_1	k_2 (g mg^{-1} min^{-1})	q_2 (mg g^{-1})	r_2
273	0.553	26.371	0.991	0.022	31.656	0.998
293	0.388	20.191	0.986	0.026	30.628	0.999
313	0.404	18.733	0.988	0.033	29.343	0.999

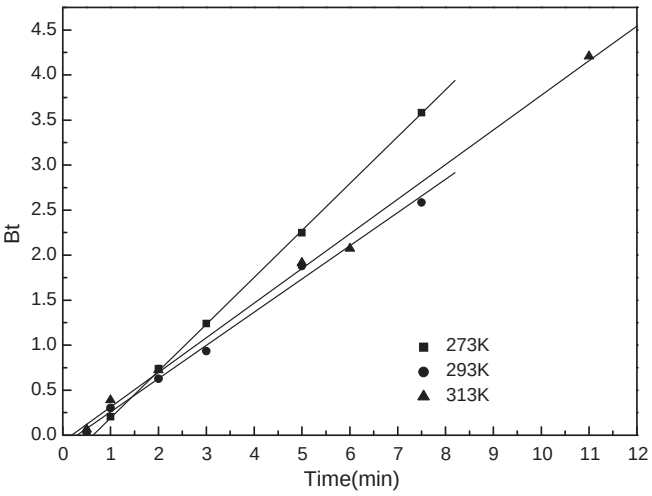

Fig. 6. Plots of Bt versus t for the adsorption of Te(IV) ions on nano-TiO_2 at different temperatures.

root of time, are shown in Fig. 7. These curves indicate that two distinct regions were observed, an initial linear part due to the boundary layer diffusion effects and a second linear part because of the intra-particle diffusion. Furthermore, the curves do not cross the origin, indicating the existence of a boundary layer resistance. The magnitude of the intercepts is proportional to the extent of the boundary layer thickness. The variation of the intercepts suggests that the mechanism of the adsorption of Te(IV) on nano-TiO_2 is predominantly diffusion controlled. Moreover, also the intra-particle diffusion plays a significant role in rate determining step. Both, the intra-particle and boundary layer diffusion are highly significant in the rate-controlling step and the values of K_{d1} and K_{d2} were obtained from the slopes of the two straight lines (K_{d1} = 9.579 mg g^{-1} min$^{-1/2}$, I_1 = 3.475, r_1 = 0.994; K_{d2} = 1.969 mg g^{-1} min$^{-1/2}$, I_2 = 20.949, r_2 = 0.891), respectively.

3.6. Adsorption isotherm and adsorption capacity

Adsorption isotherms describe how solutes interact with sorbents. In Fig. 8 the equilibrium adsorption amount of Te(IV) on nano-TiO_2 as a function of the equilibrium concentration of Te(IV) is depicted. An increased adsorption is observed for Te(IV) until saturation is attained.

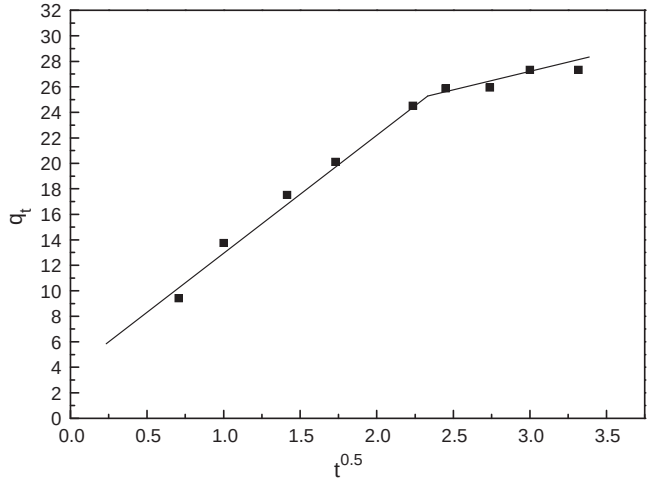

Fig. 7. Weber–Morris plots for the kinetic modeling of Te(IV) adsorption on nano-TiO_2 at room temperatures.

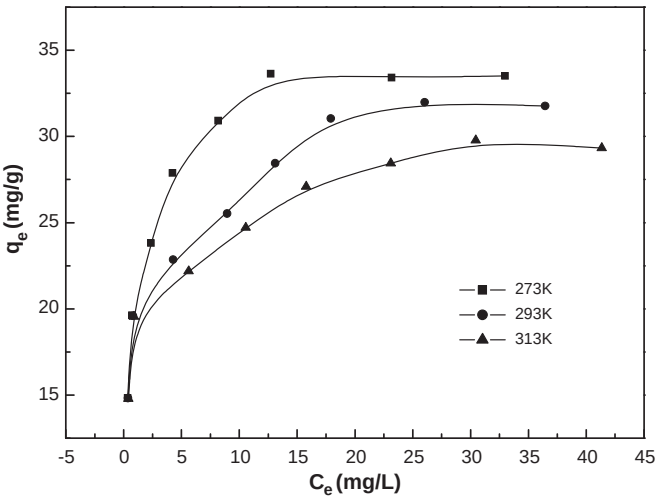

Fig. 8. Isotherm of Te(IV) adsorption on nano-TiO_2 at different temperatures (273, 293,313 K) (15 mg of nano-TiO_2; the initial Te(IV) concentration range was 30.0–90.0 mg L^{-1}; pH 8.5).

Equilibrium sorption isotherms are often described by the Langmuir model:

$$\frac{C_e}{q_e} = \frac{C_e}{q_m} + \frac{1}{bq_m} \tag{7}$$

where q_m is the maximum monolayer adsorption (mg g^{-1}), C_e is the equilibrium concentration of Te(IV), q_e is the amount of Te(IV) adsorbed per unit weight of nano-TiO_2 at equilibrium concentration (mg g^{-1}) and b is the Langmuir constant related to the affinity of binding sites (L mg^{-1}).

Furthermore, the widely used empirical Freundlich equation based on sorption on a heterogeneous surface, is given by:

$$lg\, q_e = lg\, K_F + \frac{1}{n} lg\, C_e \tag{8}$$

where K_F and n are Freundlich constants indicating the sorption capacity (mg g^{-1}) and intensity, respectively.

The Langmuir and Freundlich isothermal constants were determined from the plots of C_e/q_e against C_e, lg q_e versus lg C_e, respectively, at 273, 293 and 313 K.

The obtained isothermal constants and the correlation coefficients are presented in Table 3. It is found that the adsorption of Te(IV) on nano-TiO_2 correlated well (r > 0.99) with the Langmuir equation as compared to the Freundlich equation (r > 0.90) under the studied concentration range. The Langmuir, Freundlich isotherm constants were determined from the plots of C_e/q_e against C_e, lg q_e versus lg C_e, respectively, at 273, 293 and 313 K. Therefore, the Langmuir isotherm fits better compared with the Freundlich isotherm in all conditions according to the correlation coefficients r.

The maximum adsorption capacity of Te(IV) ions on nano-TiO_2 was 34.61, 32.75, and 30.19 mg g^{-1} at 273, 293 and 313 K, respectively.

The shape of the isotherm has been discussed with the aim to predict whether an adsorption system is favorable or unfavorable [21]. The essential feature of the Langmuir isotherms can be expressed by means of 'R_L', a dimensionless constant referred to as the separation factor or equilibrium parameter. R_L is calculated using the following equation:

$$R_L = \frac{1}{1 + bC_i} \tag{9}$$

where C_i is the initial Te(IV) concentration (mg L^{-1}) and b is the Langmuir adsorption equilibrium constant (L mg^{-1}). The calculated

Table 3
Langmuir and Freundlich constants of Te(IV) on nano-TiO_2 at the different temperatures.

T/K	Langmuir				Freundich		
	q_{max} (mg g^{-1})	b (L mg^{-1})	r	R_L	K_F (mg g^{-1})	n	r
273	34.61	1.15	0.999	0.028–0.009	19.84	5.06	0.977
293	32.75	0.82	0.997	0.039–0.013	18.52	5.90	0.985
313	30.19	0.78	0.997	0.041–0.014	17.91	6.85	0.975

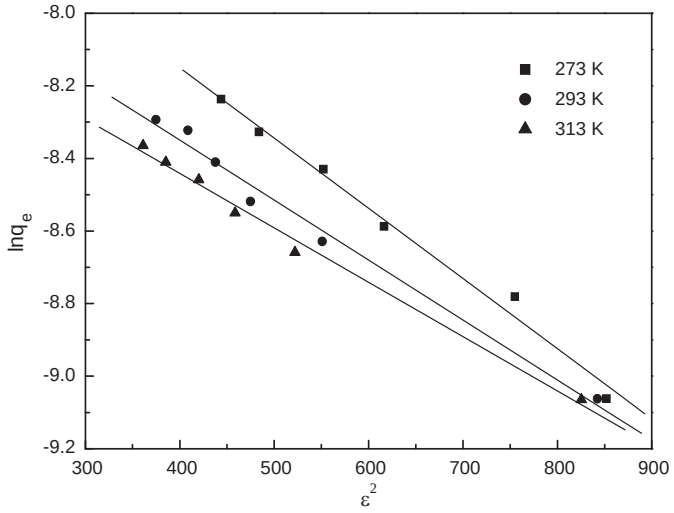

Fig. 9. D–R adsorption isotherm for Te(IV) adsorption on nano-TiO_2 at different temperatures (273, 293, 313 K) (15 mg of nano-TiO_2; the initial Te(IV) concentration range was 30.0–90.0 mg L^{-1}; pH 8.5).

R_L values are listed in Table 3. In the present investigation, the equilibrium parameter R_L was found to be in the range from 0 to 1, hence the sorption process was quite favorable and the adsorbent employed exhibited a good potential for the sorption of Te(IV).

Finally, also the Dubinin–Radushkevich (D–R) isotherm [22] was tested in its linearized form:

$$\ln q_e = \ln q_m - K\varepsilon^2 \quad (10)$$

where q_e and q_m have the same meaning as above, K is the parameter related to the adsorption energy. ε the adsorption potential, defined by Polanyi as the free energy change required to move a molecule from bulk solution to the adsorption area. The Polanyi potential varies with the concentration according to:

$$\varepsilon = RTln\left(1 + \frac{1}{C_e}\right) \quad (11)$$

where R is the ideal gas constant and T is temperature (K). A linear correlation is obtained by plotting ln q_e versus ε^2 (shown in Fig. 9), indicating that Te(IV) adsorption also obeys the D–R equation. The adsorption energy for Te(IV) adsorption can be calculated by:

$$E = (-2K)^{-1/2} \quad (12)$$

The values of the adsorption energy were evaluated as 16.09, 17.41, 18.26 kJ mol^{-1} at 273, 293 and 313 K, respectively, indicating that the value lie within the energy range for chemisorption, i.e., >16 kJ mol^{-1} [23].

3.7. Thermodynamic studies

The sorption behaviors of different concentrations Te(IV) onto nano-TiO_2 were critically investigated at 273, 293 and 313 K, respectively. Thermodynamic parameters were calculated from following equations:

$$\Delta G^0 = -RT \ln K_C \quad (13)$$

where R is the universal gas constant (8.314 J mol^{-1} K^{-1}), T is the temperature (K) and K_c is the distribution coefficient. The K_c value was calculated using following equation:

$$K_C = \frac{q_e}{C_e} \quad (14)$$

where C_e is the equilibrium concentration of Te(IV); q_e is the amount of Te(IV) adsorbed per unit weight of nano-TiO_2 at equilibrium concentration (mg g^{-1}), respectively.

The enthalpy change (ΔH^0) and entropy change (ΔS^0) of adsorption were estimated from the following equation:

$$\ln K_C = -\frac{\Delta H^0}{RT} + \frac{\Delta S^0}{R} \quad (15)$$

According to Eq. (15), ΔH^0 and ΔS^0 parameters can be calculated from the slope and intercept of the plot of ln K_c versus $1/T$, respectively.

From Eq. (13), Gibbs free energy change of adsorption (ΔG^0) was calculated using ln K_c values for different temperatures.

The values of ΔH^0, ΔS^0 and ΔG^0 were given in Table 4. The negative values of ΔH^0 and ΔG^0 showed the exothermic and spontaneous nature of sorption process.

3.8. Interference study

Under the optimum conditions, the sorption of Te(IV) ions at 30 mg L^{-1} concentration level in the presence of a large excess of diverse ions were examined. The results showed that in the presence of 1 mg mL^{-1} K^+, F^- and SiO_3^{2-}, 3 mg mL^{-1} Na^+, 150 mg mL^{-1} Ca^{2+} and Mg^{2+}, 100 mg L^{-1} SeO_3^{2-}, 200 mg L^{-1} Ba^{2+}, 550 mg L^{-1} ReO_4^- and SO_4^{2-}, 10 mg mL^{-1} NO_3^-, 3 mg mL^{-1} Cl^- and PO_4^{3-}, 20 mg mL^{-1} Br^-, 1.3 mg mL^{-1} CO_3^-, 5 mg L^{-1} Ge^{4+}, 20 mg L^{-1} Sb^{3+} the recoveries of the analytes were still above 90%. The experimental results revealed that the presence of large amounts of foreign ions in the sample has no significant effect on the separation of Te(IV). Moreover, no influence was also found for Bi^{3+}, Al^{3+}, Sn^{4+}, Mn^{2+}, Pb^{2+}, Ti^{4+}, Fe^{3+}, Cd^{2+}, Zn^{2+}, because these ions completely precipitate at pH 8.5.

Moreover, it was found that almost no adsorption for MoO_4^{2-} and WO_4^{2-} was observed on nano-TiO_2 (rutile type, shown in Table 1). So molybdenum matrix has no interference on the determination of Te(IV) in the molybdenum ore sample.

Table 4
Thermodynamic parameters for the adsorption of Te(IV) on nano-TiO_2.

C_0 (mg L^{-1})	ΔH^0 (kJ mol^{-1})	ΔS^0 (J mol^{-1} K^{-1})	ΔG^0 (kJ mol^{-1})		
			273 K	293 K	313 K
80	−13.60	−0.0418	−2.189	−1.353	−0.157

Table 5
The analytical results of the standard reference material (Mean ± S.D., $n = 7$).

Sample	Added ($\mu g\,g^{-1}$)	Found[a] ($\mu g\,g^{-1}$)	Reference value ($\mu g\,g^{-1}$)
GBW07285	0	2.9 ± 0.2	3.1 ± 0.3
	300	297.8 ± 1.3	303.1 ± 0.3

[a] Data indicate that model parameters are statistically significant (t-test) at 95% confidence level.

Table 6
Recoveries of Te(IV) in mixed standard solution and spiked water samples (Mean ± S.D., $n = 7$).

Sample	Spike ($\mu g\,mL^{-1}$)	Found[a] ($\mu g\,mL^{-1}$)	Recovery (%)
Synthetic-1	3	2.99 ± 0.23	99.7
Synthetic-2	5	4.92 ± 0.13	98.4
Synthetic-3	10	10.08 ± 0.24	100.8
Industrial wastewater	0	Not detected	–
	5	4.88 ± 0.31	97.6
	10	9.98 ± 0.22	99.8

[a] Data indicate that model parameters are statistically significant (t-test) at 95% confidence level.

3.9. Detection limits and precision

The precision of the method for processing 10 mL of 30 $\mu g\,mL^{-1}$ Te(IV) samples solution, evaluated as the relative standard deviation (R.S.D., $n = 9$) was found to be 2.0%, indicating that the method had good precision for the analysis of trace Te(IV) in solution samples. The detection limit of the method achieved, calculated on the basis of 3σ criteria (9 replicate measurements of the blank sample), is 0.013 $\mu g\,mL^{-1}$, and the quantification limit, calculated on the basis of 6σ criteria, 0.026 $\mu g\,mL^{-1}$.

3.10. Sample analysis

In order to verify the validity of the proposed method, it was applied to the determination of the content of tellurium in standard reference material (GBW07285 molybdenum ore) according to the recommended procedure. The analytical results were listed in Table 5. As can be seen, a good agreement between the determined values and the certified or reference values have been obtained.

The method was also applied to determine industrial wastewater and synthetic samples, and the analytical results along with the recoveries for the water and spiked samples were given in Table 6. The recoveries were found to be in the range of 97.6–100.8%.

4. Conclusion

In this paper, the adsorption behavior of Te(IV) ions on nano-TiO_2 was investigated. The main advantages of the procedure are its ease and straightforwardness, and the fast creation of the phase equilibration. The experimental results indicate that nano-TiO_2 can effectively separate Te(IV) ions from aqueous solutions in the pH range of 1–2 and 8–9, and has very high adsorption capacity for Te(IV) ions. The adsorption percentage of Te(IV) exceeds 97%. Kinetic studies suggest that the equilibrium is achieved within 8 min and a pseudo-second-order is followed. The overall rate process appears to be influenced by both boundary layer diffusion and intra-particle diffusion. The adsorption isotherms could be well fitted applying the Langmuir and Dubinin–Radushkevich equations. Furthermore, the adsorption process was found to be exothermic, spontaneous under the conditions studied. The results clearly prove that adsorption of Te(IV) on nano-TiO_2 is an economical, viable and high efficient way for separating Te(IV) from aqueous solutions. Finally, nano-TiO_2 sorbents was successfully applied to the separation and determination of inorganic tellurium ions from water samples, and geological samples with complex matrix.

Acknowledgements

This work was financially supported by the Science Foundation of Education Department of Liaoning Province and the Natural Science Foundation of Liaoning Province, China (Nos. 20082050, 2007T053 and 2009R30). The authors also thank colleagues and other students who participated in this work.

References

[1] Z.F. Chai, H.M. Zhu, Introduction to Trace Element Chemistry, Atomic Energy Press, Peking, China, 1994, pp. 201–204.
[2] I.S. Balogh, V. Andruch, Anal. Chim. Acta 386 (1999) 161–167.
[3] X.K. Wang, Y.P. Li, Chem. Propellants Polym. Mater. 1 (2003) 11–13.
[4] J.M. Rajwade, K.M. Paknikar, Hydrometallurgy 71 (2003) 243–248.
[5] I. Harezov, N. Jordanov, Talanta 21 (1974) 1013–1024.
[6] T. Sekine, Y. Hasegawa, Solvent Extraction Chemistry: Fundamentals and Applications, Marcel Dekker, New York, 1977, pp. 632–635.
[7] W.C. Cooper, Tellurium, Van Nostrand Reinhold, New York, 1971, pp. 281–285.
[8] G.S. Desai, V.M. Shinde, Talanta 39 (1992) 405–408.
[9] A. Ramesh, M.S. Subramanian, Bull. Chem. Soc. Jpn. 71 (1998) 1025–1033.
[10] Y.V. Ghalsasi, S.S. Khopkar, V.M. Shinde, Indian J. Chem. 38A (1999) 621–629.
[11] L. Zhang, T. Huang, N. Liu, X.Y. Liu, H.M. Li, Microchim. Acta 165 (2009) 73–78.
[12] L. Zhang, N. Lui, L.J. Yang, Q. Lin, J. Hazard. Mater. 170 (2009) 1197–1203.
[13] H.F. Feng, J.Y. Yin, G.Y. Yang, Yunnan Metallurgy 28 (1999) 41–42.
[14] W.M. Wang, V. Fthenakis, J. Hazard. Mater. 125 (2005) 80–88.
[15] D.C. MCPHAIL, Geochim. Cosmochim. Acta 59 (1995) 851–866.
[16] A. Mizuike, Enrichment Techniques for Inorganic Trace Analysis, Springer-Verlag, Berlin, New York, 1983, pp. 6–8.
[17] S. Azizian, J. Colloid Interface Sci. 276 (2004) 47–52.
[18] M.S. Shaukat, M.I. Sarwar, R. Qadee, J. Radioanal. Nucl. Chem. 265 (2005) 73–79.
[19] R. Qadeer, Colloids Surf. A 293 (2007) 217–223.
[20] V.S. Mane, I.D. Mall, V.C. Srivastava, J. Environ. Manage. 84 (2007) 390–400.
[21] W.S.W. Ngah, A. Kamari, Y. Koay, Int. J. Biol. Macromol. 34 (2004) 155–161.
[22] A. Kilislioglu, B. Bilgin, Appl. Radiat. Isot. 58 (2003) 155–160.
[23] G.M. Xu, Z. Shi, J. Deng, Chin. J. Environ. Eng. 1 (2007) 15–18.